Cholecystokinin B Receptor Antagonists for the Treatment of Depression via Blocking Long-term Potentiation in the Basolateral Amygdala

Jufang He (✉ jufanghe@cityu.edu.hk)

City University of Hong Kong

Xu ZHANG

city university of hong kong

Muhammad Asim

Md Monir Hossain

Kyuhee Kim

Wei Fang

Hemin Feng

Shujie Wang

Qianqian Gao

Yuanying Lai

Article

Abstract

Depression is a common mental disorder. Evidence suggested a substantial causal relationship between stressful life events and the onset of episodes of major depression. Here, we investigated how CCK and CCKBR in the basolateral amygdala (BLA) are implicated in stress-mediated depressive-like behavior. The BLA mediates emotionally charged memory and long-term potentiation (LTP) is a trace of memory. Cholecystokinin knockout (CCK-KO) mice lacked LTP in the BLA; while the application of CCK4 induced LTP after low-frequency stimulation (LFS). Optogenetic activation of CCK fibers from the entorhinal cortex (EC) to BLA promoted stress susceptibility. CCK-B receptor knockout (CCKBR-KO) mice showed LTP deficits in the BLA; CCKBR antagonists blocked high-frequency stimulation (HFS) induced LTP in the BLA. CCK-KO and CCKBR-KO mice showed significantly lower levels of depression-related behaviors than wild-type control mice. Notably, CCKBR antagonists displayed a reduction in depressive-like behaviors in the acute tail suspension test (TST) and open field test (OFT), chronic social defeat stress (CSDS) model of mice. Together, these results indicate that CCKBR is a potential target to treat depression.

Introduction

Depression is a leading cause of disability and a major contributor to the overall global burden of disease (WHO 2021), affecting more than 280 million people worldwide (GHDx). Most current antidepressant drugs have side effects and delayed onset of action (Ferguson 2001, Birmes, Coppin et al. 2003, Mitchell 2006, Csoka, Bahrick et al. 2008). Therefore, developing new antidepressants with a specific novel target and with no or minimal side effects becomes increasingly important for society.

Considerable evidence suggests that stressful events or experiences may increase the risk of depression (Kessler 1997, Hammen 2005); Kendler indicated the substantial causal relationship between stressful life events and the onset of episodes of major depression (Kendler, Karkowski et al. 1999). Emotionally charged memory is associated with the amygdala (Cahill, Babinsky et al. 1995), and depression is correlated with the hyperactivated amygdala (Siegle, Thompson et al. 2007, Peluso, Glahn et al. 2009, Yang T T 2010).

Cholecystokinin (CCK) has long been recognized as a neuropeptide involved in depression (Hernando, Fuentes et al. 1994, Löfberg, Ågren et al. 1998, Becker, Zeau et al. 2008, Del Boca, Lutz et al. 2012). A clinical study of 105 patients suffering from major depression showed that patients who had made one or more suicide attempts tended to have higher cerebrospinal fluid (CSF) CCK levels than those who had not (Löfberg, Ågren et al. 1998). The previous study indicated that CCKBR antagonist L-365,260 exhibited antidepressant effects in forced swim tests of mice (Hernando, Fuentes et al. 1994). Moreover, a CCKBR antagonist CI-988 prevented chronic social defeat induced depressive behaviors and increased cortical CCK release in the rat model (Becker, Zeau et al. 2008). Although these studies showed that the CCK and CCKBR are implicated in depression, the mechanism of how CCK involves in depression and the mechanism of antidepressant effects of CCKBR antagonists remains unclear.

Observations that patients with medial temporal lobe (MTL) damage show deficits in forming new long-term memories of facts and events (Scoville and Milner 1957) have led to our current understanding that the MTL is essential for establishing enduring declarative memories (Squire and Zola-Morgan 1991), spatial memory (Bohbot, Iaria et al. 2004, Glikmann-Johnston, Saling et al. 2008) and emotionally charged memory (Dolcos, LaBar et al. 2004, Buchanan, Tranel et al. 2006). CCK is the most abundant neuropeptide in the brain (REHFELD and JF 1978). Mice lacking the CCK gene exhibit poor performance in passive avoidance tasks and display impaired spatial (Lo, Samuelson et al. 2008), associative and fear memories (Chen, Li et al. 2019, Feng, Su et al. 2021). The MTL sends a "plasticity-enabled" signal to the neocortex to switch on the encoding of new associations, evidence suggests that the plasticity-enabled signal is CCK from the EC (Chen, Guo et al. 2013, Li, Yu et al. 2014, Chen, Li et al. 2019). No LTP, the physiological trace of memory, was induced in the neocortex of CCK-KO mice, while it was readily induced in their wild-type control (Chen, Li et al. 2019). The BLA mediates fear conditioning, and recent evidence implicates that the CCK projection neurons in the EC enable LTP and fear memory-encoding in the lateral amygdala (LA) using CCK as the chemical signal (Feng, Su et al. 2021). CCKBR antagonist blocks theta-burst stimulation (TBS) induced LTP in the neocortex (Chen, Li et al. 2019). The amygdala shows abundant CCKBR expression (Honda, Wada et al. 1993, Feng, Su et al. 2021). We hypothesized that CCK might facilitate aversive memory formation by enabling LTP in the BLA, enhancing the development of depression. CCKBR antagonists would suppress the formation and consolidation of aversive memories, leading to the treatment of depression by blocking LTP in the amygdala.

In the present study, we tested the above hypotheses by using in vitro recording, optogenetic manipulation, histology, and behavioral analysis. First, we examined whether CCK could switch LTP formation in the BLA via? Then it was examined whether optogenetic activation of CCK projections from EC-BLA can promote stress susceptibility? Next, we investigated the effects of CCKBR antagonists on neural plasticity in the BLA. Finally, the antidepressant effects of CCKBR antagonists were tested on the mouse model and compared with current antidepressants.

Results

CCK signaling is critical for LTP induction in the BLA.

As emotionally charged memory is associated with neuronal activity or neuroplasticity in the amygdala (Cahill, Babinsky et al. 1995), we first examined the dependency of CCK signaling in LTP induction in the BLA.

We adopted a brain-slice electrophysiological system with multiple slices and microelectrode arrays (**fig.1 a**) to compare the LTP induction in the BLA between the CCK-KO mice and its wild-type control. CCK-KO mice showed a deficit in TBS induced LTP in the BLA, as compared to their wild-type controls (two-way RM ANOVA, significant interaction, $F_{[1,20]}$ = 19.7, p = 2.5E-4 < 0.001; pairwise comparison, post hoc Bonferroni test; first 10 min before vs. last 10 min after the TBS in CCK-KO mice, 100.5 ± 0.3% vs. 112.4 ±

2.8%, P > 0.05; first 10 min before vs. last 10 min after the TBS in wild-type mice, 100.4 ± 0.5% vs. 161.4 ± 8.9%, P = 1.0E-7 < 0.001, **fig.1 d**).

It is known that LFS does not induce LTP in the field-potential recording setting. LFS induces long-term depression (LTD) when both the number of stimulation pulses (typically 900 pulses) and the current of stimulation are large (Collingridge, Peineau et al. 2010). As previously reported, we concluded that HFS induced the release of CCK from the presynaptic terminals, leading to LTP in the neocortex and amygdala (Chen, Li et al. 2019, Feng, Su et al. 2021). We then hypothesize that the application of the CCKBR agonist (CCK4) induces LTP in the BLA even under the LFS paradigm.

Application of CCK4 with LFS (100 pulses) induced LTP in the BLA, whereas application of the vehicle did not (two-way RM ANOVA, significant interaction, $F_{[1,18]}$ = 6.6, p = 0.02 < 0.05; pairwise comparison, post hoc Bonferroni test; with vehicle, first 10 min before vs. last 10 min after LFS, 99.4 ± 0.5% vs. 108.2 ± 4.6%, P > 0.05 ; with CCK4, first 10 min before vs. last 10 min after LFS, 99.4 ± 0.97% vs. 196.9.2 ± 34.6%, P = 0.005 < 0.01, **fig.1 e**). Both the loss-of-function and gain-of-function studies supported the critical role of CCK signaling in LTP induction or neuroplasticity in the BLA.

Figure 1. CCK signaling is critical in LTP induction in the BLA. a. Workflow of in-vitro recording and CCK4 administration, after 15min baseline recording, perfused artificial cerebrospinal fluid (ACSF) diluted with CCK4 for 5min with LFS, then fresh ACSF washed out CCK4 after. **b.** Light microscopy photograph showing the location of a 4*4 microelectrode array placed on the BLA region. **c.** Schematic diagram of TBS and LFS. **d.** Time courses of field excitatory postsynaptic potentials (fEPSPs) changes in response to TBS of wild-type mice (WT) and CCK-KO mice in the BLA (left). Representative fEPSPs traces before (gray) and after LTP induction (right). **e.** Time courses of fEPSPs changes in response to CCK4/vehicle with LFS in the BLA of WT mice (left). Representative fEPSPs traces before (gray) and after LTP induction (right). All data are the mean ± SEM.

Optogenetic activation of the ECcck−BLA pathway promoted stress susceptibility.

CCK signaling is critical in neuroplasticity in the amygdala. The fear memory can be inactivated and reactivated by LTD and LTP (Nabavi, Fox et al. 2014). Recently, we found that activating CCK-positive projection from the EC to LA by a high-frequency laser stimulation modulated the neuronal plasticity, and potentiated auditory response in LA neurons (Feng, Su et al. 2021). We implanted an optical fiber in the BLA after virus injection into the EC of CCK-Cre mice (AAV-EF1a-DIO-ChETA-EYFP in the experimental group, ChETA; AAV-EF1a-DIO- EYFP in the control group, EYFP; **fig. 2 a b).** To test whether CCK from the EC to BLA enhances the development of depression, we adopted the two-trial subthreshold social defeat stress (SSDS) model behaviorally. As described previously (Chaudhury, Walsh et al. 2013, Shen, Zheng et al. 2019), an intruder CCK-Cre mouse was introduced into the home cage of an aggressive novel resident CD1 mouse for 10 min physically defeat, then, they were maintained in sensory contact for 10 min. After a 5 min interval, the second trial was carried out.During the sensory stress phases of SSDS, we applied

bilateral intra-BLA high-frequency laser stimulation (HFLS, 20HZ, duration 5ms, 600 pulses) to activate the ECcck-BLA projections (**fig. 2 c**).

We confirmed the injection site of the AAV virus in the EC and their projections in the BLA (**fig. 2 d**). The duration spent in the social interaction zone when a novel social target was present in the SI test showed no difference in the two groups (two-way RM ANOVA, $F_{[1,26]}$ = 0.40, p > 0.05; pairwise comparison, post hoc Bonferroni test; target phase, ChETA vs. EYFP, 52.6 ± 13.0s vs. 52.9 ± 8.0s, P > 0.05, **fig. 2 e**). However, the preference for sucrose solution of the ChETA group reduced significantly, compared with that of the control mice (two-sample t-test, ChETA vs. EYFP, 66.9 ± 3.9% vs. 78.1 ± 2.7%, t = -2.4, P = 0.02 < 0.05, **fig. 2 f**). These results indicated that the activation of CCK projections from the EC to BLA facilitated stress susceptibility and induced anhedonia phenotype, a loss of capability to perceive pleasure, one of the most stringent parameters in depression.

Figure 2. Optogenetic activation of the ECcck–BLA in SSDS induced depressive behaviors. a. The workflow of the SSDS model with optogenetic manipulation. Day 1, virus injection into the bilateral EC of CCK-Cre mice. Day 28, fibers implantation to the bilateral BLA. Day 35, SSDS paradigm with optogenetic activations. Day 36, SI, SPT. Day 43, BLA tissue collection for the immunohistochemistry (IHC) test. **b.** Schematic diagram of virus injection of EC and optical fiber implantation of BLA. **c.** Paradigms of 20 Hz optogenetic activation of CCK fibers in the EC-BLA circuit during two sensory phases of SSDS. **d.** CHETA-EYFP or EYFP was specifically expressed in CCK neurons at EC (up) and projections to BLA (bottom), scale bar, 500 μm. **e.** Schematic diagram of SI (left). Time that mice spent in social interaction zone, two-way RM ANOVA, pairwise comparison, post hoc Bonferroni test (right). **f.** Sucrose preference percentage in the SPT, two-sample t-test. * P < 0.05, **P < 0.01, ***P < 0.001, n.s., not significant. All data are the mean ± SEM.

CSDS activated CCKBR neurons at BLA.

Activity in the amygdala is higher when a person is sad or clinically depressed (Schneider, Grodd et al. 1997, Peluso, Glahn et al. 2009, Yang T T 2010). The CSDS is a widely accepted model for depression study (Golden, Covington et al. 2011). In the next experiment, we examined if CSDS could induce the hyperactivated amygdala. As CCKBRs are expressed intensively in the amygdala (Honda, Wada et al. 1993, Feng, Su et al. 2021), we examined whether the activated neurons correlate with CCKBRs.

We adopted a 10-day protocol of CSDS in depression induction in the mice (**supplementary fig. 1 a**). The time spent in the social interaction zone in the presence of a social target of the mice who underwent the CSDS is significantly less than that of sham group mice (two-way RM ANOVA, $F_{[1,13]}$ = 4.49, p = 0.05; pairwise Comparison, post hoc Bonferroni test; with the target, CSDS vs. sham, 64.1.8 ± 2.3s vs. 106.8 ± 4.6s, P = 0.03 < 0.05; **supplementary fig. 1 c**). We measured c-Fos and CCKBR expression in the BLA when the mice were re-exposed to novel CD1 mice. Notably, c-Fos expression in the BLA was significantly higher than in the sham group mice (two-sample test, t = -7.0, P = 1.9E-7 < 0.001; **supplementary fig. 1 d-e**). Furthermore, 91.5 ± 2.1% of c-Fos-positive neurons activated by stress in CSDS mice were colocalized

with CCKBR neurons (**supplementary fig. 1 f**). These results indicated that CCKBR correlated with the hyperactivation of the BLA of CSDS mice.

CCKBR antagonist suppressed LTP induction in the BLA

Previously, we have shown that CCKBR antagonists block the LTP induction in the neocortex and the encoding of sound-sound and visuoauditory associative memory (Li, Yu et al. 2014, Chen, Li et al. 2019). Here, we investigated the role of CCKBR in LTP induction in the BLA with brain-slice preparation.

Transgenic mice lacking the CCKBR gene (CCKBR-KO) exhibited a deficit of TBS-induced LTP in the BLA, as compared to their wild-type (WT, 129S1 mice) control (two-way RM ANOVA, significant interaction, $F_{[1,17]}$ = 24.4, p = 1.2E-4 < 0.001; pairwise comparison, post hoc Bonferroni test; in CCKBR-KO mice, first 10 min before vs. last 10 min after TBS, 100.0 ± 0.3% vs. 102.7 ± 2.4% , P = 0.57 > 0.05; in WT mice, first 10 min before vs. last 10 min after TBS, 99.8 ± 0.5% vs. 135.4 ± 6.0%, P = 2.1E-6 < 0.001, **fig. 3 b**).

A natural question was whether a CCKBR antagonist could block or suppress the LTP induction in the BLA. YM022 is a selective CCKBR antagonist, with an IC50 for CCKBR of 68 pM vs 63 nM for CCKAR (Nishida, Miyata et al. 1994). Perfusion of YM022 (1 nM/10 nM) suppressed the LTP induction in the BLA of C57 mice, whereas perfusion of the vehicle did not (two-way RM ANOVA, significant interaction, $F_{[2, 23]}$ = 9.78, P = 8.4E-4 < 0.001; pairwise comparison, post hoc Bonferroni test; with vehicle, first 10 min before vs. last 10 min after TBS, 99.20 ± 0.3% vs. 172.3 ± 18.0%, P = 3.9E-6 < 0.001; 1 nM of YM022, first 10 min before vs. last 10 min after TBS, 99.6 ± 0.9% vs. 122.1 ± 2.8%, P > 0.05; 10 nM of YM022, first 10 min before vs. last 10 min after TBS, 99.6 ± 0.4% vs. 110.2 ± 5.6%, P > 0.05; last 10 min after TBS, between groups, vehicle vs. 1 nM of YM022, 172.3 ± 18.0% vs. 122.1 ± 2.8%, p = 8.5E-4 < 0.001, vehicle vs. 10 nM of YM022, 172.3 ± 18.0% vs. 110.2 ± 5.6%, P = 2.3E-5 < 0.001, **fig. 3 c**).

Another selective CCKBR antagonist YF476 with an IC50 for CCKBR of 0.1 nM vs 502 nM for CCKAR (Semple, Ryder et al. 1997) , 10nM of YF476 fully blocked TBS-induced LTP in the BLA of C57 mice (two-way RM ANOVA, significant interaction, $F_{[1, 18]}$ = 14.6, P = 0.001; pairwise comparison, post hoc Bonferroni test ; for YF476, first 10 min before vs. last 10 min after TBS, 101.0 ± 0.7% vs. 106.5 ± 9.0%, P > 0.05; for vehicle, first 10 min before vs. last 10 min after TBS, 101.1 ± 0.8% vs. 187.5 ± 17.4%, P = 2.67E-5 < 0.001; last 10 min after TBS, between groups, vehicle vs. YF476, 187.5 ± 17.4% vs. 106.5 ± 9.0%, P = 1.1E-4 < 0.001, **supplementary fig. 2 b**).

Figure 3. LTP deficit in CCKBR-KO mice and YM022 blocked LTP in the BLA. a. Workflow of in-vitro recording and drug administration, after 15min baseline recording, perfused ACSF diluted with drug for 10min, then fresh ACSF washed out drug after TBS. **b.** Time courses of fEPSPs changes in response to TBS of wild-type mice (WT) and CCKBR-KO mice in the BLA (left). Representative fEPSPs traces before (gray) and after LTP induction (right). **c.** Time courses of fEPSPs changes of C57 wild-type mice (WT) in response to YM022/vehicle with TBS in the BLA (left). Representative fEPSPs traces before (gray) and after LTP induction (right). All data are the mean ± SEM.

CCKBR-KO and CCK-KO transgenic mice demonstrated lower levels of depression-like behaviors

Before testing CCKBR antagonists in the behavioral animal model, we examined how CCKBR-KO and CCK-KO mice performed in the TST and FST in terms of the total immobility time. The shorter total immobility time indicates less despair behavior, indicating less depression-like activity (Vincent Castagn´e 2010). The CCKBR-KO mice had significantly less immobility time in the FST and TST than the wild-type (ICR mice) (**fig. 4 b-c**; CCKBR-KO vs. wild-type, in FST, 118.8 ± 17.3s vs.197.4 ± 12.3s, two-sample t-test, t = 3.7, P = 0.002 < 0.01; in TST, 67.1 ± 15.5s vs. 131.8 ± 21.2s, two-sample t-test, t = 2.5, P = 0.02 < 0.05). However, no significant difference in immobility times was observed in the FST and TST for the CCK-KO mice compared with the wild-type background (**supplementary fig 3. a b**; CCK-KO vs. wild-type, in FST, 180.7 ± 4.3s vs. 185.8 ± 3.6s, two-sample t-test, t = 0.9, P > 0.05; in TST, 186.1 ± 15.6s vs. 208.6 ± 16.1s, two-sample t-test, t =1.0, P > 0.05).

The OFT is the most widely used technique to investigate the anxiolytic or anxiogenic effects of pharmacological compounds (Seibenhener and Wooten 2015). Compared with WT mice, the CCKBR-KO mice spent significantly more time in the center zone (**fig. 4 d**, CCKBR-KO vs. wild-type, 17.7 ± 1.2% vs.12.4 ± 1.1%, two-sample t-test, t = -3.3, P = 0.005 < 0.01), and traveled significantly more distance (**fig. 4 e**, CCKBR-KO vs. wild-type, 49.6 ± 1.8m vs. 29.1 ± 1.8m, two-sample t-test, t = -8.0, P = 1.4E-6 < 0.001) and defecated significantly fewer feces than the wild-type in the open field (**fig. 4 f**, CCKBR-KO vs. wild-type, 1.7 ± 0.5 vs. 5.4 ± 0.6, two-sample t-test, t = 4.8, P = 2.9E-4 < 0.001). Notably, the CCK-KO mice spent significantly more time in the central area than their wild-type control (**supplementary fig. 3 d**, CCK-KO vs. wild-type, 5.8 ± 1% vs. 2.4 ± 0.5%, two-sample t-test, t= -3.0, P = 0.01 < 0.05). We observed no significant difference in fecal boil deposits and total distance in the OFT (**supplementary fig 3. e f**: CCK-KO vs. wild-type, total distance, 17.5 ± 0.8m vs. 17.5 ± 1.5m, two-sample t-test, t = 0.007, P > 0.05; fecal boil, 3.6 ± 0.9 vs. 4.9 ± 0.7, two-sample t-test, t = 1.0, P > 0.05). In summary, the CCKBR-KO and CCK-KO mice showed a lower level of anxiety-like behavior as compared with their WT controls.

Figure 4. Antidepressant-related behavioral responses of CCKBR-KO mice and antidepressant effect of YM022 in acute stress model. a. Schematic of the TST and FST. **b.**Total immobility time in the last 4 min of the FST. wild-type mice (WT, N= 8) vs. CCKBR-KO mice (N=9), two-sample t-test. **c.** Total immobility time in 6 min of the TST, WT(N= 8) vs. CCKBR-KO (N=9), two-sample t-test. **d-g.** The anxiolytic behavior of CCKBR-KO mice (N=7) in the OFT, WT group (N=9). **d.** Time percentage spent in the center percentage, two-sample t-test. **e.** Total distance traveled, two-sample t-test. **f.** Fecal deposits, two-sample t-test. **g.** Representative traces in OFT (5min). **h.** YM022 administration 30 min before TST test by IP injection. **i,** Total immobility time in 6 min of the TST, saline group (N=16); YM022 groups, 0.3 µg/kg (N= 9), 0.6 µg/kg (N= 10), 3.0 µg/kg (N= 10), 30 µg/kg (N= 10), fluoxetine 10mg.kg (N= 10), one-way ANOVA, pairwise comparison, post hoc Bonferroni test. **j.** YM022 administration 30 min before the OFT test by IP injection. **k-m.** The anxiolytic effect of YM022 (3.0ug/kg, N=10) in the OFT, vehicle group (N=9). **k.** Time percentage spent in the center, two-sample t-test. **i.** Total distance traveled in the OFT, two-sample t-test. **m.** Representative traces in OFT (10min test time).* P < 0.05, **P < 0.01, ***P < 0.001, n.s., not significant. All data are the mean ± SEM.

Blood-brain barrier penetration of CCKBR antagonists, YM022 and YF476

Depression is associated with the hyperactivity of the amygdala (Mayo_Clinic , Siegle, Thompson et al. 2007, Peluso, Glahn et al. 2009, Yang T T 2010). Most c-Fos expressed neurons in the BLA after CSDS were CCKBR positive neurons. CCKBR mediates the CCK signaling of EC-LA projections and LTP in the BLA. Our previous study demonstrated that the EC-LA CCK projection enabled the association between the auditory cortex and the amygdala, linking the fear memory with the sensory signal (Feng, Su et al. 2021). Up to this point, it is reasonable to examine whether CCKBR antagonists can alleviate the depression symptoms, by suppressing the LTP induction that encodes/consolidate aversive memory in the BLA. To show an antidepressant-like response, a drug must cross the blood-brain barrier (BBB) so that it can reach the target. According to Pardridge, around 98% of small molecules cannot penetrate the blood-brain barrier (BBB) and work on the CNS [20]. Before we apply the CCKBR antagonists, YM022 and YF476, for behavioral assay, we examined their BBB permeability and pharmacokinetics.

After single oral administration of YM022 (5 mg/kg) and YF476 (5 mg/kg), the plasma and brain samples were obtained at the several time points after dosing: 15, 30 min, and 1, 2, 4, 6, 8, 24 hours, and analyzed by LC-MS/MS analysis (**supplementary fig. 4 a**). The peak concentration of YM022 in brain tissue was 6.0 ± 1.8 ug/L at 30min post-dose; pharmacokinetic profiles of YM022 in the plasma showed that maximum concentration(C_{max}) was 215.2 ug/L, time for C_{max} to occur (T_{max}) was 0.38 hour, half-life ($T_{1/2}$) was 1.3 hours, and area under the plasma concentration-time curve AUC (0-∞) was 321.8 ug/L*h (**supplementary fig. 4 b-c**). The peak concentration of YF476 in brain tissue was 32.7 ± 6.8 ug/L at 15min post-dose; pharmacokinetic parameters of YF476 in plasma C_{max} was 341.5 ug/L, T_{max} was 0.38 hour, $T_{1/2}$ was 0.5 hours, and AUC (0-∞) was 228.1 ug/L*h (**supplementary fig. 4 d-e**). The results indicated that YM022 and YF476 can penetrate the BBB.

CCKBR antagonists showed antidepressant effects in the acute TST and OFT

Determination of the total immobility time (despair behavior) in the TST allows a quick assessment of potential antidepressant effects, various classes of antidepressant drugs decrease immobility time in the TST. (Cryan, Mombereau et al. 2005, Vincent Castagn´e 2010). We examined the effects of acute administration of CCKBR antagonists on the duration of immobility in the TST.

We compared the effects of the CCKBR antagonists, YM022 and YF476, with the saline control and current antidepressant, fluoxetine (a selective serotonin receptor inhibitors, SSRIs) as the positive control. The fluoxetine at a dose of 10 mg/kg significantly decreased the total immobility time in the TST; of four different concentrations of YM022 (0.3 µg/kg, 0.6 µg/kg, 3.0 µg/kg, and 30 µg/kg) that were tested, mice showed a considerable less immobility time with doses of 0.6 µg/kg and 3.0 µg/kg (**fig. 4 i,** one-way ANOVA, $F_{[5,59]}$ = 5.6, P = 2.81E-4 < 0.001; means comparisons, post hoc Bonferroni test; fluoxetine vs. saline, 92.2 ± 15.8s vs. 192.3 ± 16.9s, P = 0.001 < 0.01; for YM022, 0.3 µg/kg vs. saline, 186.1 ± 14.3s vs.192.3 ± 16.9s, P > 0.05, 0.6 µg/kg vs. saline, 117.6 ± 13.6s vs.192.3 ± 16.9s, P = 0.035 < 0.05, 3.0µg/kg vs. saline, 118.1 ± 13.4s vs.192.3 ± 16.9s, P = 0.038 < 0.05, 30µg/kg vs. saline, 132.3 ± 26.3s vs.192.3 ±

16.9s, P > 0.05). Moreover, mice treated with YF476 also showed a significant decreased immobility time with a doses of 1.3 μg/kg and 3.0 μg/kg (one-way ANOVA, $F_{[4,45]}$ = 9.0, P = 2.0E-5 < 0.001, means comparisons, post hoc Bonferroni test; for YF476, 0.3 μg/kg vs. saline, 231.3 ± 13.6s vs. 195 ± 11.3s, P > 0.05, 1.3 μg/kg vs. saline, 111.1 ± 15.4s vs. 195 ± 11.3s, p = 0.012 < 0.05, 3.0μg/kg vs. saline, 114.8 ± 21.7s vs. 195 ± 11.3s, p = 0.024 < 0.05, 30μg/kg vs. saline, 137.9 ± 23.2s vs. 195 ± 11.3s, p > 0.05, **supplementary fig. 5 b**). As the period of immobility is an indicator of hopelessness during the TST test, CCKBR antagonists, both YM022 and YF476, demonstrated a similar beneficial effect as compared to fluoxetine a positive control.

Next, we adopted the OFT to evaluate the anxiolytic effect of YM022. We administrated intraperitoneally YM022 (3.0 ug/kg) 30 min before the OFT. We observed no difference in the total distance traveled between vehicle and YM022 treated mice during the 10-min test time (**fig. 4 l,** vehicle vs. YM022, 63.6 ± 4.3m vs. 63.3 ± 2.8m, two-sample t-test, t = 0.06, P > 0.05), but YM022 treated mice spent significantly more time in the center (**fig. 4 k,** vehicle vs. YM022, 14.9 ± 0.86% vs. 18.8 ± 1.4%, two-sample t-test, t = -2.4, P = 0.03 < 0.05). This result revealed that CCKBR antagonist YM022 has anxiolytic effects at the dose of 3.0 ug/kg.

Figure 4. Antidepressant-related behavioral responses of CCKBR-KO mice and antidepressant effect of YM022 in acute stress model. a. Schematic of the TST and FST. **b.** Total immobility time in the last 4 min of the FST. wild-type mice (WT, N= 8) vs. CCKBR-KO mice (N=9), two-sample t-test. **c.** Total immobility time in 6 min of the TST, WT(N= 8) vs. CCKBR-KO (N=9), two-sample t-test. **d-g.** The anxiolytic behavior of CCKBR-KO mice (N=7) in the OFT, WT group (N=9). **d.** Time percentage spent in the center percentage, two-sample t-test. **e.** Total distance traveled, two-sample t-test. **f.** Fecal deposits, two-sample t-test. **g.** Representative traces in OFT (5min). **h.** YM022 administration 30 min before TST test by IP injection. **i.** Total immobility time in 6 min of the TST, saline group (N=16); YM022 groups, 0.3 μg/kg (N= 9), 0.6 μg/kg (N= 10), 3.0 μg/kg (N= 10), 30 μg/kg (N= 10), fluoxetine 10mg.kg (N= 10), one-way ANOVA, pairwise comparison, post hoc Bonferroni test. **j.** YM022 administration 30 min before the OFT test by IP injection. **k-m.** The anxiolytic effect of YM022 (3.0ug/kg, N=10) in the OFT, vehicle group (N=9). **k.** Time percentage spent in the center, two-sample t-test. **l.** Total distance traveled in the OFT, two-sample t-test. **m.** Representative traces in OFT (10min test time).* P < 0.05, **P < 0.01, ***P < 0.001, n.s., not significant. All data are the mean ± SEM.

Antidepressant effects of CCKBR antagonists in the CSDS model

Finally, we used the CSDS to examine whether CCKBR antagonists have a possible antidepressant effect. We administrated YM022 30 min before each physical defeat to prevent the development of depressive-like behavior in mice. We conducted SI and SPT respectively, 24 hours after the final social defeat(**fig 5. a**).

YM022 (3.0 μg/kg) and positive control fluoxetine (10mg/kg) treated mice spent significantly more time at the social interaction zone with the social target than vehicle treated mice (**fig 5. b,** two-way RM ANOVA

, $F_{[3,78]}$ = 7.5, p = 1.9E-4 < 0.001; pairwise comparison, post hoc Bonferroni test; target phase, vehicle vs. sham, 58.5 ± 5.6s vs. 79.8.8 ± 3.4s, p = 0.058, vehicle vs YM022, 58.5 ± 5.6s vs. 79.3 ± 5.3s, p = 0.03 < 0.05, vehicle vs fluoxetine, 58.5 ± 5.6s vs. 88.8 ± 6.2s, p = 7.28148E-4 < 0.001), and the social interaction ratio in drug treated group is also increased significantly (**fig 5. c,** one-way ANOVA, $F_{[3,78]}$ = 5.49, P = 0.002 < 0.01; means comparison, post hoc Bonferroni test; vehicle vs. sham, 0.99 ± 0.11 vs. 1.6 ± 0.1, P = 0.003 < 0.01, vehicle vs. YM022, 0.99 ± 0.11 vs. 1.47 ± 0.1; P = 0.02 < 0.05, vehicle vs fluoxetine, 0.99 ± 0.11 vs. 1.5 ± 0.15, P = 0.026 < 0.05).

Besides, it has been found that only the vehicle group mice spent significantly more time in corners than the sham, YM022, and fluoxetine treated mice, to actively avoid the novel social target (**fig 5. d**, two-way RM ANOVA, $F_{[3,78]}$ = 8.83, p = 4.1E-5 < 0.001; pairwise comparison, post hoc Bonferroni test; vehicle vs. sham , 35.8 ± 5.2s vs. 16.1 ± 1.6s, P = 5.9E-4 < 0.001, vehicle vs. YM022, 35.8 ± 5.2s vs. 15.9 ± 2.9s, p = 1.34E-4 < 0.001, vehicle vs. fluoxetine, 35.8 ± 5.2s vs. 17.0 ± 3.2s p = 0.002 < 0.01). The corner ratio showed a significant difference accordingly (**fig 5. e,** one-way ANOVA, $F_{[3,78]}$ = 13.7, P =2.9E-7 < 0.001; means comparison, post hoc Bonferroni test; vehicle vs. sham, 2.15 ± 0.29 vs. 0.73 ± 0.09, P = 1.9E-5 < 0.001, vehicle vs YM022, 2.2 ± 0.29 vs. 0.65 ± 0.14, P = 9.95E-7< 0.001, vehicle vs fluoxetine, 2.2 ± 0.29 vs. 0.93 ± 0.16, P = 3.6E-4 < 0.001).

Consistent with social interaction behavior results, sham, YM022, and fluoxetine groups consumed significantly more sucrose liquid than vehicle group mice (**fig 5. g**, one-way ANOVA, $F_{[3,78]}$ = 8.25734 , P = 7.7E-5 < 0.001; means comparison, post hoc Bonferroni test; vehicle vs. sham, 66.9 ± 1.7% vs. 78.9 ± 1.8%, P = 4.6E-5 < 0.001, vehicle vs YM022, 66.9 ± 1.7% vs. 74.4 ± 1.8%, P = 0.01 < 0.05, vehicle vs fluoxetine, 66.9 ± 1.7% vs. 74.6 ± 1.6%, P = 0.019 < 0.05).

These results demonstrated that CCKBR antagonist YM022 effectively prevented CSDS-induced social avoidance and anhedonia in mice.

Figure 5. Antidepressant effects of YM022 in CSDS model. **a.** The workflow of CSDS with vehicle/YM022(3ug/kg)/fluoxetine(10mg/kg) injection 30min before every social defeat (left) and sham group(right). **b.** Time spent in social interaction zone in the absence and presence of a social target. Two-way RM ANOVA, pairwise comparison, post hoc Bonferroni test. **c.** Social interaction ratio = time spent in the social interaction zone with target/time spent in the social interaction zone without a target. One-way ANOVA, pairwise comparison, post hoc Bonferroni test. **d.** The time that mice spent in corners in the absence and presence of a social target. Two-way RM ANOVA, pairwise comparison, post hoc Bonferroni test. **e.** Corner ratio = time spent in the corner with target/time spent in the corner without a target, One-way ANOVA, pairwise comparison, post hoc Bonferroni test. **f.** Representative sample track traces of social interaction test no-target phase (top), and the target phase (bottom). **g.** Sucrose preference percentage in SPT. One-way ANOVA, pairwise comparison, post hoc Bonferroni test. *P < 0.05, **P < 0.01, ***P < 0.001, n.s., not significant. All data are the mean ± SEM.

Discussion

Despite the clinical (Löfberg, Ågren et al. 1998) and preclinical studies (Hernando, Fuentes et al. 1994, Becker, Zeau et al. 2008) reporting the critical role of cholecystokinin and its receptor in a depression state, less attention has been paid to understanding how CCK and CCKBR involved in the depression. In this study, we combined the in vitro electrophysiological recording, optogenetic manipulation, c-fos & CCKBR staining, and behavioral analysis to examine the critical role of CCK and CCKBR application in depression. By comparing the degree of EPSPs from CCK-KO, CCKBR-KO, and wild-type control mice, we provided a critical role of CCK and CCKBR in the induction of LTP. We identified that CCKBR antagonist YM022 prevents the development of depressive-like behavior.

A substantial causal relationship between stressful life events and the onset of episodes of major depression (Kendler, Karkowski et al. 1999). Much evidence from animal studies has proved that LTP in the amygdala mediates emotional learning and memory (Cahill, Babinsky et al. 1995, Maren 1999). Amygdala receives all sensory inputs by linking with the olfactory bulbs, thalamus, and cortical areas et al (LeDoux 2007), and ties emotional response to meaningless environmental stimuli (LeDoux 2003, LeDoux 2007). Recent studies demonstrated the prominent role of hyperactivated BLA (Siegle, Thompson et al. 2007, Peluso, Glahn et al. 2009, Yang T T 2010) and dysregulation of connectivity with the downstream anatomical targets in the depression (Liu, Ota et al. 2015) (Shen, Zheng et al. 2019) (Ma, Li et al. 2021). Stress activates the input from BLA to the medial prefrontal cortex (mPFC) and ketamine treatment would ameliorate it in chronic stress and major depression (Liu, Ota et al. 2015). The circuit of BLA to the nucleus accumbens modulates depressive-like behavior when experiencing stress (Shen, Zheng et al. 2019). BLA-hippocampal innervation modulates stress-induced depressive-like behaviors through AMPA receptors (Ma, Li et al. 2021).

Synaptic plasticity has been conventionally accepted as the cellular substrate of learning and memory. Although the extent to which synaptic plasticity constitutes the cellular substrate of a particular behavioral phenotype is still under debate ((Josselyn and Tonegawa 2020, Wu, Ramos et al. 2021), it may serve as the substrate of depression. Previously, we have shown that CCKKO mice lack HFS-induced LTP and puffing CCK4 with low frequency induced the LTP in the auditory cortex (Chen, Li et al. 2019). Consist with our previous study, in this study we found the same phenomenon in the BLA. Furthermore, we found that CCKBR-KO mice lack LTP. Notably, CCKBR antagonists YM022 and YF476 block the TBS-induced LTP. Thus, these results conclude that the CCK and CCKBR are critically implicated in the LTP induction in the BLA. Future studies need to elucidate if synaptic plasticity in the BLA could act as a potential antidepressant target.

Rodent depression models demonstrated several behavioral phenotypes observed in depressive patients, including anxiety, despair, anhedonia, and social avoidance (Duman 2010, Planchez, Surget et al. 2019). In the present study, we adopted the acute TST, FST, and OFT model and chronic CSDS model to assess depression-like behaviors. We used the TST to screen the effective doses of candidate compounds as an antidepressant (**Fig. 4i, supplementary Fig. 4b**). A previous study revealed that chronic but not acute treatment of fluoxetine reversed CSDS induced social avoidance (Berton, McClung et al. 2006). Here, the antidepressant effects of our drug candidate were reconfirmed by the CSDS model, which mimics human

depression happening. Acute combined chronic depression behavioral testing platforms could extend the spectrum of assessing the drug effects in the animal model, which might be not easy to assess in the human subjects.

Regardless of the considerable effort of pharmaceutical companies for decades, no CCKBR antagonist has been developed into a drug, solubility and oral bioavailability are two such reasons. Because of poor systemic availability, CI-988 (CCKBR antagonist) demonstrated a relatively modest effect on CCK4-induced panic symptoms in healthy volunteers (Bradwejn, Koszycki et al. 1995). In the present study, we examined PK parameters and BBB penetration of the CCKBR antagonists, YM022 and YF476, and found the parameters were acceptable.

A recent study showed that CCK-KO mice have deficient trace fear memory formation and neural plasticity deficit in the LA (Feng, Su et al. 2021). Here it was tested that CCKBR antagonists YM022 and YF476 blocked TBS-induced LTP in the BLA (**Fig. 3c, supplementary Fig. 2**). The current study looks at depression from a new angle by suppressing the formation and/or consolidation of the aversive memory. We focused on CCKBRs that mediate the neuroplasticity signal, enabling the formation and consolidation of aversive memory in the amygdala. It is striking that the CCKBR antagonists have similar anti-depression effects as the current SSRIs, proposing a novel target for pharmaceutical intervention. The other worth-mentioning result is that YM022 demonstrated an effective antidepressant effect at a 3333.3-fold lower dosage than the fluoxetine (**Fig. 5**). Together, our findings demonstrate that CCKBR antagonists may suppress depression by blocking the LTP.

Methods

Animals. All experimental procedures were reviewed and approved by the Animal Subjects Ethics Sub-Committees of the City University of Hong Kong. The following transgenic mice were used: CCK-ires-Cre (Ccktm1.1(Cre)Zjh/J, C57 background, abbreviated CCK-Cre, Jackson Laboratory), CCKBR-KO (ICR background), CCKBR-KO (Cckbrtm1Kpn/J, 129S1 background, abbreviated CCKBR-KO, Jackson Laboratory), and CCK-CreER (Ccktm2.1(Cre/ERT2)Zjh/J, stock# 012710, C57 background, abbreviated CCK-KO, Jackson Laboratory), the corresponding wild-type background mice were also used. Especially, The CCKBR-KO and 129 background mice have involved in vitro electrophysiological recording; and CCKBR-KO and ICR background were involved in behavioral experiments. C57BL/6 male adult (SLAC) mice (7weeks of age) were used to establish the CSDS model of depression from the same vendor, the Chinese University of Hong Kong. All behavioral tests were carried out during the dark phase. Mice were housed in a 12-hour light/12-hour dark cycle (dark from 9:00 to 21:00) and given food and water ad libitum.

Viral injection and optical fiber implantation. The following viruses were used: AAV-Ef1a-DIO-ChETA-EYFP (a gift from Karl Deisseroth, Addgene viral prep # 26968-AAV9; http://n2t.net/addgene:26968; RRID: Addgene_26968) and AAV-EF1a-DIO-EYFP (BrainVTA, Wuhan, China). All virus preparations were diluted to the appropriate titer (approximately 1.6×10^{13} VG/ml) with 5% glycerol before injection. CCK-Cre mice

were anesthetized by pentobarbital sodium (50 mg/kg, i.p. injection). A mouse was fixed in a stereotaxic device, and a scalp incision was made. A local anesthetic (xylocaine, 2%) was applied to the incision site for analgesia. For viral injection in the entorhinal cortex, the coordinate is as follows: AP=4.25 mm, ML=3.85 mm, and DV=2.55 mm from the surface, with volume=400 nL. For optical fiber implantation of the BLA, the coordinates are AP=1.60 mm, ML=3.45 mm, and DV=3.65 mm from the surface. Craniotomy was performed after skull leveling, and the dura mater was partially opened by a syringe needle hook (29G). We used a Nanoliter Injector from WPI (World Precision Instruments, Sarasota County, FL) for virus infusion. A glass pipette filled with a virus was gently inserted to the desired depth from the dura surface. The virus was slowly pumped into brain tissue at a speed of no more than 50 nL/min. After infusion, the pipette was placed in the injection site for an extra 5–10 min before withdrawing slowly. After the injection, the scalp was sutured, and a local anesthetic was applied. Then, the animal was returned to the home cage after awakening. For optogenetic axon stimulation, the virus was expressed for at least five weeks in our experiment. For optical fiber implantation, the fibers were gently inserted into the coordinate of BLA and fixed with dental cement (mega PRESS NV + JET X, megadental GmbH, Büdingen, Germany).

In vitro electrophysiology. ACSF was prepared with the following protocol: 124 mM NaCl, 2.5 mM KCl, 1 mM NaH2PO4, 10 mM D glucose, 25 mM NaHCO3, 2 mM CaCl2, and 1 mM MgCl2, at pH 7.35-7.45. Before use, ACSF was well oxygenated (95% O2/5% CO2, v/v).For brain slices preparation, animals were deeply anesthetized with isoflurane. Coronal sections (thickness, 300 μm) across the objective brain region, the amygdala, were cut in well-oxygenated ice-cold ACSF using a vibratome.

The brain slices were allowed to recover for 1.5 h at 30 ± 1°C in oxygenated ACSF. After recovery, one slice was positioned on the microelectrode array system probe (MED-PG515A) on the stage of the microscope. Once the slice was settled, a fine mesh and anchor were carefully overlaid on the slices to ensure stabilization during recording. Then, the slices were continuously perfused with oxygenated 30 ± 1°C ACSF with the aid of a peristaltic pump during electrophysiological recording. The 4*4 channel microelectrode array was located on the targeted brain region under a light microscope. One microelectrode was selected for stimulation, referring to the microscope photo. For the selection of the best stimulation site, monopolar, biphasic constant-current pulses (0.2 ms in duration) were generated by Mobius software with a 2 s interval. The fEPSPs were evoked at several of the remaining sites. The fEPSPs were amplified by an amplifier and displayed on the monitor screen. Microelectrodes were screened, and the best stimulation site was selected. After 30 min of recovery of the slices with stabilization of the baseline fEPSP responses, an input-output curve was determined by using the measurements of the fEPSPs amplitude (output) in response to a series of ascending stimulation intensities in 10 mA steps (input). For LTP induction, 30–50% saturated intensity was selected as the stimulation intensity for the baseline synaptic response recording. fEPSPs responded stably for at least 15 min set as a baseline. Then, a TBS protocol (4 sets with 10 s intervals, each set consisting of 5 trains at 5 Hz, 4 pulses at 100 Hz as one train) was given at the stimulation site. The stimulation intensity of TBS was adjusted to elicit 75% of the saturated intensity to introduce LTP. For the drug effects test, after baseline recording, perfused ACSF diluted with CCKBR antagonist (YM022 or YF476) for 10min before

TBS; or perfused ACSF diluted with CCKBR agonist (CCK4) for 5min with LFS (75% of the saturated intensity,1HZ, 100 pulses), then fresh ACSF washed out drug after TBS/LFS. fEPSP responses were recorded for at least 60 min after TBS/LFS. Changes in the fEPSP amplitudes were analyzed as a percentage change from the baseline. The average normalized amplitudes of the first 10 min before and the last 10 min after TBS/LFS were compared. For comparison of the LTP magnitude between groups, the averaged values of the last 10 min were compared statistically.

Immunochemistry. Mice were deeply anesthetized with pentobarbital (100 mg/kg, i.p. injection) and perfused transcardially with 20 ml of phosphate-buffered saline (PBS) followed by 20 ml of 4% paraformaldehyde (PFA) in 0.1 MPBS, pH 7.4. Brains were removed and postfixed overnight in 4% PFA at 4°C in 0.1 M PBS. Coronal sections (thickness; 50 μm) were cut in 0.1 M PBS using a vibratome and stored at -20°C in an antifreeze solution (50% PBS, 20% ethylene glycol, 30% glycerin). Targeted slices across the amygdala (-1.70 mm relative to the bregma) were selected under a light microscope and washed three times with PBS. The slices were incubated in a blocking solution for 1.5 hours at room temperature. Blocking solution prepared with the following: 5% normal goat serum, 0.2% Triton X-100, with PBS. Then, the slices were shaken with primary antibodies in a blocking solution overnight at 4°C. The primary antibodies used were c-Fos (1:1000, ab208942) and CCKBR (1:1000, PA3-201). After three washes with PBS, sections were incubated with Alexa Fluor 594 (1:500), and Alexa Fluor 488 (1:1000) secondary antibodies at room temperature for three hours. After another three 7 min washes in PBS, immunofluorescence was assessed using a Ni-E upright fluorescence microscope (Nikon). The percentage of c-Fos/CCKBR colocalized neurons in each group was calculated as the percentage of the total number of c-Fos/CCKBR colocalized neurons counted within the total number of c-Fos-expressing neurons counted.

Chronic social defeat stress (CSDS) model of depression. It was performed as described previously (Golden, Covington et al. 2011). Retired breeder male CD1 mice were screened on three consecutive days to validate their aggressive characteristics. During ten days of the chronic social defeat stress procedure for the experimental group, male intruder C57 mice were introduced into the resident CD1 mouse home cage. The novel aggressive CD1 mice physically attacked the C57 mice for 10 min. After that, using a perforated acrylic board partition, the resident cage was divided into two, wherein the residents and intruders could be maintained in sensory contact for 24 h. For 10 successive days, a C57 mouse was introduced to a novel aggressive CD1 mouse cage every day. After ten days of CSDS, the animals were housed singly, and social interaction behavior was tested 24 h later. For the sham group, two C57 mice were housed in one cage separated by a perforated acrylic partition. A novel partner was rotated every day, and physical contact with each other was avoided.

Two-trial subthreshold social defeat stress (SSDS) model. It was performed as described previously (Chaudhury, Walsh et al. 2013, Shen, Zheng et al. 2019). Before the trial, retired resident breeder CD1 mice were screened for aggressive behavior. In a two-trial social defeat experiment, an intruder CCK-Cre mouse was placed into the home cage of an aggressive novel resident CD1 mouse for 10 min physical defeat. Then, with a perforated acrylic board partition dividing the resident home cage

into two, residents and intruders maintained sensory contact for 10 min. After 10 min of the sensory stress phase, the CCK-Cre mouse was returned to its home cage for 5 min. Then, the second round of 10 min of physical defeat and 10min sensory stress in the home cage of another novel CD1 mouse was carried out. After two defeat tails, the intruder CCK-Cre was returned to its home cage and accepted the social interaction test the following day.During the sensory stress phase, bilateral intra-BLA laser stimulation stimulated the EC-BLA circuit. The laser power was adjusted to 10 mW before each experiment. For ChETA-mediated stimulation, the optical fibers were connected to a 473 nm blue laser diode.

Social interaction test (SI). The social interaction behavior of mice that underwent social defeat was tested in an open-field arena ($44 \times 44 \times 44$ cm^3) containing an empty acrylic cage ($9.5 \times 9.5 \times 8$ cm^3). The social interaction test included no target and target phases. In the no target stage, a mouse was placed in the center of the open field arena facing the empty acrylic cage for 2.5 min. The animals' track was analyzed with Smart.3 video-tracking software, and the time spent in the social interaction zone surrounding the acrylic cage (a 6 cm region around) was measured. The animal was then returned to the home cage for 1 min. In the target stage, a novel, aggressive CD1 mouse was placed in the acrylic cage, and the same metric was measured. From these two stages, a social interaction ratio was calculated (the time spent in the interaction zone in the target phase/the time spent in the interaction zone in no target phase).

Sucrose preference test (SPT). Animals that underwent CSDS or SSDS were singly housed and habituated with two 50 ml tubes of water for 1 week before social defeat stress and 1 day before SPT. Then, the experimental animals were given access to one tube of water and one tube of 1% sucrose solution for 24 hours and were weighed at 10:00, 15:00, and 18:00. The bottle position (left or right) was switched after each weight measurement to avoid a side preference. The sucrose preference ratio was calculated by dividing the total consumption of sucrose solution by the total consumption of both water and sucrose solution.

Tail suspension test (TST). Mice were suspended by their tails with adhesive tape (1 cm from the tail tip) approximately 50 cm above the surface. Acrylic board partitioning was applied to ensure no contact. Plastic tubes were placed over the tail to ensure that the mice could neither climb nor hang on to their tails. The animals were video recorded from the side for 6 min, and the total immobility time was quantitated by Smart.3 video-tracking software over the full 6 min post hoc.

Forced swimming test (FST). Mice were individually placed into a cylinder of water ($23°C \pm 1°C$, 16 cm diameter × 24 cm high) for 6 min. The water depth was set to prevent animals from touching the bottom with their tails or hind limbs. Animal behavior was video recorded from the side. The total immobility time of the last 4min was quantitated by Smart.3 video-tracking. The immobility of the mice was defined as remaining floating or motionless, with only movements necessary to maintain the balance in the water.

Open field test (OFT). Mice were individually introduced to the central zone of an open field (50 cm length, 50 cm width, 40 cm height) with dim light for 5/10 min. Their exploration in the arena was recorded by a video camera and analyzed by Smart 3.0 software. Locomotor activity was evaluated as the total distance traveled. The anxiety-like behavior level was defined by the time spent in the center region (central 30*30 cm zone). The number of fecal boli deposited accounted for anxiety after the test.

Drug delivery. For the acute behavior test, the drug was administered by i.p. injection 30 min before the test.For drug delivery in the CSDS model, C57 mice were treated with 10 mg/kg fluoxetine or 3.0ug/kg YM022 once a day via i.p. injection for ten days. Control C57 mice received the vehicle of the YM022 injection. The injection site changed left or right daily.

Pharmacokinetics. Materials and instrument: MS2 Turnover type oscillator was purchased from IKA Work's Guangzhou (China), and a 5415Rhigh speed tabletop centrifuge was purchased from Eppendorf AG (Germany). Chromatographic analyses were performed with an HPLC system consisting of an LC-10ADvp Pump (SHIMADZU, Japan), and an MPS3C automatic sample (Gerstel Autosampler, Germany), and API3000 triple quadrupole tandem mass spectrometer (AB co., U.S.). Propranolol (≥90% in purity, internal standard, IS) was purchased from Sigma Chemical Co. (China). Formic acid (HPLC grade) and methanol (HPLC grade) were purchased from DIKMA Co. (China). All chemicals and solvents were analytical grades. And the water was purified using a Millipore (AK, USA) laboratory ultra-pure water system (0.2μm filter). Animal: Male KM mice, weighing 32-36g (Southern China Medical University, China) were utilized for the studies. The protocol was approved by the Animal Care and Use Committee, GIBH. Animals were maintained on standard animal chow and water ad libitum, in a climate-controlled room(23±1°C, 30–70% relative humidity, a minimum of 10 exchanges of room air per hour, and a 12-h light/dark cycle) for one week before experiments. Pharmacokinetic studies: The compound was dissolved in the solution containing 2% DMSO, 4% ethanol, 4% castor oil, and 90% DD H2O; Pharmacokinetic properties of mice (male) were determined following PO administration. Animals were randomly distributed into 8 experimental groups (n = 4). The mice were given 5 mg/kg (YM022 YF476) by gastric gavage. The dosing volume was 10 ml/kg (PO). After single administration, whole blood (100 μL) and brain samples were obtained at the following time points after dosing: 15, 30 min, and 1, 2, 4, 6, 8, and 24 hours (PO group). Whole blood and brain samples were collected in heparinized tubes. The plasma fraction was immediately separated by centrifugation (8,000 rpm, 6 min, and 4 °C) and all samples were stored at −20 °C until LC-MS-MS analysis. Plasma sample analysis: standard curve sample preparation. The compound was dissolved in DMSO at a concentration of 2mg/mL and diluted with 100% acetonitrile solution to series concentration. 10μL series concentration solution and 50μL blank plasma /50gm blank brain were added to 1.5mL tube and vortex for 3min, then 150μL acetonitrile containing internal standard was added and vortex for 5min, finally spin tube in the centrifuge at 16000g for 40min at 4°C, the final concentration was as follow: 2, 5, 10, 20, 50, 100, 200, 500, 1000, 2000, 5000ng/mL. Plasma preparation: The plasma /brain samples were prepared using the protein precipitation method. 10μL acetonitrile solution and 50μL plasma samples were added to 1.5mL tube and vortex for 3min, then 150μL acetonitrile containing internal standard was added and vortex for 5mins, finally spin tube in the centrifuge at 16000g for 40min at 4°C. LC-MS analysis: After centrifuge,

100μL supernatant was transferred to the 96 well plates and analyzed by LC-MS/MS using an Applied Biosystems-SCIEX model API 3000 mass spectrometer. Pharmacokinetics parameters: The pharmacokinetic parameters were calculated by analyzing the compound concentration in plasma samples using the pharmacokinetic software DAS.2.0

Declarations

References

1. Becker, C., B. Zeau, C. Rivat, A. Blugeot, M. Hamon and J. J. Benoliel (2008). "Repeated social defeat-induced depression-like behavioral and biological alterations in rats: involvement of cholecystokinin." Mol Psychiatry 13(12): 1079–1092.

2. Berton, O., C. A. McClung, R. J. DiLeone, V. Krishnan, W. Renthal, S. J. Russo, D. Graham, N. M. Tsankova, C. A. Bolanos and M. Rios (2006). "Essential role of BDNF in the mesolimbic dopamine pathway in social defeat stress." Science 311(5762): 864–868.

3. Birmes, P., D. Coppin, L. Schmitt and D. Lauque (2003). "Serotonin syndrome: a brief review." Cmaj 168(11): 1439–1442.

4. Bohbot, V. D., G. Iaria and M. Petrides (2004). "Hippocampal function and spatial memory: evidence from functional neuroimaging in healthy participants and performance of patients with medial temporal lobe resections." Neuropsychology 18(3): 418.

5. Bradwejn, J., D. Koszycki, M. Paradis, P. Reece, J. Hinton and A. Sedman (1995). "Effect of CI-988 on cholecystokinin tetrapeptide-induced panic symptoms in healthy volunteers." Biological psychiatry 38(11): 742–746.

6. Buchanan, T. W., D. Tranel and R. Adolphs (2006). "Memories for emotional autobiographical events following unilateral damage to medial temporal lobe." Brain 129(1): 115–127.

7. Cahill, L., R. Babinsky, H. J. Markowitsch and J. L. McGaugh (1995). "The amygdala and emotional memory." Nature 377(6547).

8. Chaudhury, D., J. J. Walsh, A. K. Friedman, B. Juarez, S. M. Ku, J. W. Koo, D. Ferguson, H.-C. Tsai, L. Pomeranz and D. J. Christoffel (2013). "Rapid regulation of depression-related behaviours by control of midbrain dopamine neurons." Nature 493(7433): 532–536.

9. Chen, X., Y. Guo, J. Feng, Z. Liao, X. Li, H. Wang, X. Li and J. He (2013). "Encoding and retrieval of artificial visuoauditory memory traces in the auditory cortex requires the entorhinal cortex." Journal of Neuroscience 33(24): 9963–9974.

10. Chen, X., X. Li, Y. T. Wong, X. Zheng, H. Wang, Y. Peng, H. Feng, J. Feng, J. T. Baibado and R. Jesky (2019). "Cholecystokinin release triggered by NMDA receptors produces LTP and sound–sound associative memory." Proceedings of the National Academy of Sciences 116(13): 6397–6406.

11. Collingridge, G. L., S. Peineau, J. G. Howland and Y. T. Wang (2010). "Long-term depression in the CNS." Nat Rev Neurosci 11(7): 459–473.

12. Cryan, J. F., C. Mombereau and A. Vassout (2005). "The tail suspension test as a model for assessing antidepressant activity: review of pharmacological and genetic studies in mice." Neurosci Biobehav Rev 29(4–5): 571–625.

13. Csoka, A., A. Bahrick and O.-P. Mehtonen (2008). "Persistent sexual dysfunction after discontinuation of selective serotonin reuptake inhibitors." The journal of sexual medicine 5(1): 227–233.

14. Del Boca, C., P. Lutz, J. Le Merrer, P. Koebel and B. Kieffer (2012). "Cholecystokinin knock-down in the basolateral amygdala has anxiolytic and antidepressant-like effects in mice." Neuroscience 218: 185–195.

15. Dolcos, F., K. S. LaBar and R. Cabeza (2004). "Interaction between the amygdala and the medial temporal lobe memory system predicts better memory for emotional events." Neuron 42(5): 855–863.

16. Duman, C. H. (2010). "Models of depression." Vitamins & Hormones 82: 1–21.

17. Feng, H., J. Su, W. Fang, X. Chen and J. He (2021). "The entorhinal cortex modulates trace fear memory formation and neuroplasticity in the mouse lateral amygdala via cholecystokinin." Elife 10: e69333.

18. Ferguson, J. M. (2001). "SSRI antidepressant medications: adverse effects and tolerability." Primary care companion to the Journal of clinical psychiatry 3(1): 22.

19. GHDx. (2019). " Institute of Health Metrics and Evaluation, Global Health Data Exchange (GHDx)." from http://ghdx.healthdata.org/gbd-results-tool?params=gbd-api-2019-permalink/d780dffbe8a381b25e1416884959e88b

20. Glikmann-Johnston, Y., M. M. Saling, J. Chen, K. A. Cooper, R. J. Beare and D. C. Reutens (2008). "Structural and functional correlates of unilateral mesial temporal lobe spatial memory impairment." Brain 131(11): 3006–3018.

21. Golden, S. A., H. E. Covington, O. Berton and S. J. Russo (2011). "A standardized protocol for repeated social defeat stress in mice." Nature protocols 6(8): 1183–1191.

22. Hammen, C. (2005). "Stress and depression." Annu. Rev. Clin. Psychol. 1: 293–319.

23. Hernando, F., J. Fuentes, B. P. Roques and M. Ruiz-Gayo (1994). "The CCKB receptor antagonist, L-365,260, elicits antidepressant-type effects in the forced-swim test in mice." European journal of pharmacology 261(3): 257–263.

24. Honda, T., E. Wada, J. F. Battey and S. A. Wank (1993). "Differential gene expression of CCKA and CCKB receptors in the rat brain." Molecular and Cellular Neuroscience 4(2): 143–154.

25. Josselyn, S. A. and S. Tonegawa (2020). "Memory engrams: Recalling the past and imagining the future." Science 367(6473): eaaw4325.

26. Kendler, K. S., L. M. Karkowski and C. A. Prescott (1999). "Causal relationship between stressful life events and the onset of major depression." American Journal of Psychiatry 156(6): 837–841.

27. Kessler, R. C. (1997). "The effects of stressful life events on depression." Annual review of psychology 48(1): 191–214.

28. LeDoux, J. (2003). "The emotional brain, fear, and the amygdala." Cellular and molecular neurobiology 23(4): 727–738.

29. LeDoux, J. (2007). "The amygdala." Current biology 17(20): R868-R874.

30. Li, X., K. Yu, Z. Zhang, W. Sun, Z. Yang, J. Feng, X. Chen, C.-H. Liu, H. Wang and Y. P. Guo (2014). "Cholecystokinin from the entorhinal cortex enables neural plasticity in the auditory cortex." Cell Research 24(3): 307–330.

31. Liu, R. J., K. T. Ota, S. Dutheil, R. S. Duman and G. K. Aghajanian (2015). "Ketamine Strengthens CRF-Activated Amygdala Inputs to Basal Dendrites in mPFC Layer V Pyramidal Cells in the Prelimbic but not Infralimbic Subregion, A Key Suppressor of Stress Responses." Neuropsychopharmacology 40(9): 2066–2075.

32. Lo, C.-M., L. C. Samuelson, J. B. Chambers, A. King, J. Heiman, R. J. Jandacek, R. R. Sakai, S. C. Benoit, H. E. Raybould and S. C. Woods (2008). "Characterization of mice lacking the gene for cholecystokinin." American Journal of Physiology-Regulatory, Integrative and Comparative Physiology 294(3): R803-R810.

33. Löfberg, C., H. Ågren, J. Harro and L. Oreland (1998). "Cholecystokinin in CSF from depressed patients: possible relations to severity of depression and suicidal behaviour." European neuropsychopharmacology 8(2): 153–157.

34. Ma, H., C. Li, J. Wang, X. Zhang, M. Li, R. Zhang, Z. Huang and Y. Zhang (2021). "Amygdala-hippocampal innervation modulates stress-induced depressive-like behaviors through AMPA receptors." Proc Natl Acad Sci U S A 118(6).

35. Maren, S. (1999). "Long-term potentiation in the amygdala: a mechanism for emotional learning and memory." Trends in neurosciences 22(12): 561–567.

36. Mayo_Clinic. "PET scan of the brain for depression." from https://www.mayoclinic.org/tests-procedures/pet-scan/multimedia/-pet-scan-of-the-brain-for-depression/img-20007400.

37. Mitchell, A. J. (2006). "Two-week delay in onset of action of antidepressants: new evidence." The British Journal of Psychiatry 188(2): 105–106.

38. Nabavi, S., R. Fox, C. D. Proulx, J. Y. Lin, R. Y. Tsien and R. Malinow (2014). "Engineering a memory with LTD and LTP." Nature 511(7509): 348–352.

39. Nishida, A., K. Miyata, R. Tsutsumi, H. Yuki, S. Akuzawa, A. Kobayashi, T. Kamato, H. Ito, M. Yamano and Y. Katuyama (1994). "Pharmacological profile of (R)-1-[2, 3-dihydro-1-(2'-methylphenacyl)-2-oxo-5-phenyl-1H-1, 4-benzodiazepin-3-yl]-3-(3-methylphenyl) urea (YM022), a new potent and selective gastrin/cholecystokinin-B receptor antagonist, in vitro and in vivo." Journal of Pharmacology and Experimental Therapeutics 269(2): 725–731.

40. Peluso, M. A., D. C. Glahn, K. Matsuo, E. S. Monkul, P. Najt, F. Zamarripa, J. Li, J. L. Lancaster, P. T. Fox, J. H. Gao and J. C. Soares (2009). "Amygdala hyperactivation in untreated depressed individuals." Psychiatry Res 173(2): 158–161.

41. Planchez, B., A. Surget and C. Belzung (2019). "Animal models of major depression: drawbacks and challenges." Journal of Neural Transmission 126(11): 1383–1408.

42. REHFELD, J. F. and R. JF (1978). "Immunochemical studies on cholecystokinin. II. Distribution and molecular heterogeneity in the central nervous system and small intestine of man and hog."

43. Schneider, F., W. Grodd, U. Weiss, U. Klose, K. R. Mayer, T. Nägele and R. C. Gur (1997). "Functional MRI reveals left amygdala activation during emotion." Psychiatry Research: Neuroimaging 76(2–3): 75–82.

44. Scoville, W. B. and B. Milner (1957). "Loss of recent memory after bilateral hippocampal lesions." Journal of neurology, neurosurgery, and psychiatry 20(1): 11.

45. Seibenhener, M. L. and M. C. Wooten (2015). "Use of the Open Field Maze to measure locomotor and anxiety-like behavior in mice." J Vis Exp(96): e52434.

46. Semple, G., H. Ryder, D. P. Rooker, A. R. Batt, D. A. Kendrick, M. Szelke, M. Ohta, M. Satoh, A. Nishida and S. Akuzawa (1997). "(3 R)-N-(1-(tert-Butylcarbonylmethyl)-2, 3-dihydro-2-oxo-5-(2-pyridyl)-1 H-1, 4-benzodiazepin-3-yl)-N '-(3-(methylamino) phenyl) urea (YF476): A Potent and Orally Active Gastrin/CCK-B Antagonist." Journal of medicinal chemistry 40(3): 331–341.

47. Shen, C. J., D. Zheng, K. X. Li, J. M. Yang, H. Q. Pan, X. D. Yu, J. Y. Fu, Y. Zhu, Q. X. Sun, M. Y. Tang, Y. Zhang, P. Sun, Y. Xie, S. Duan, H. Hu and X. M. Li (2019). "Cannabinoid CB1 receptors in the amygdalar cholecystokinin glutamatergic afferents to nucleus accumbens modulate depressive-like behavior." Nat Med 25(2): 337–349.

48. Siegle, G. J., W. Thompson, C. S. Carter, S. R. Steinhauer and M. E. Thase (2007). "Increased amygdala and decreased dorsolateral prefrontal BOLD responses in unipolar depression: related and independent features." Biological psychiatry 61(2): 198–209.

49. Squire, L. R. and S. Zola-Morgan (1991). "The medial temporal lobe memory system." Science 253(5026): 1380–1386.

50. Vincent Castagn´e, P. M., Sylvain Roux, and Roger D. Porsolt (2010). "Rodent model of depression forced swim and tail suspension behaviral despair tests in rats and mice."

51. WHO. (2021). "Depression ", from https://www.who.int/news-room/fact-sheets/detail/depression.

52. Wu, C.-H., R. Ramos, D. B. Katz and G. G. Turrigiano (2021). "Homeostatic synaptic scaling establishes the specificity of an associative memory." Current Biology 31(11): 2274–2285. e2275.

53. Yang T T, S. A. N., Matthews S C, et al (2010). "Adolescents With Major Depression Demonstrate Increased Amygdala activation."
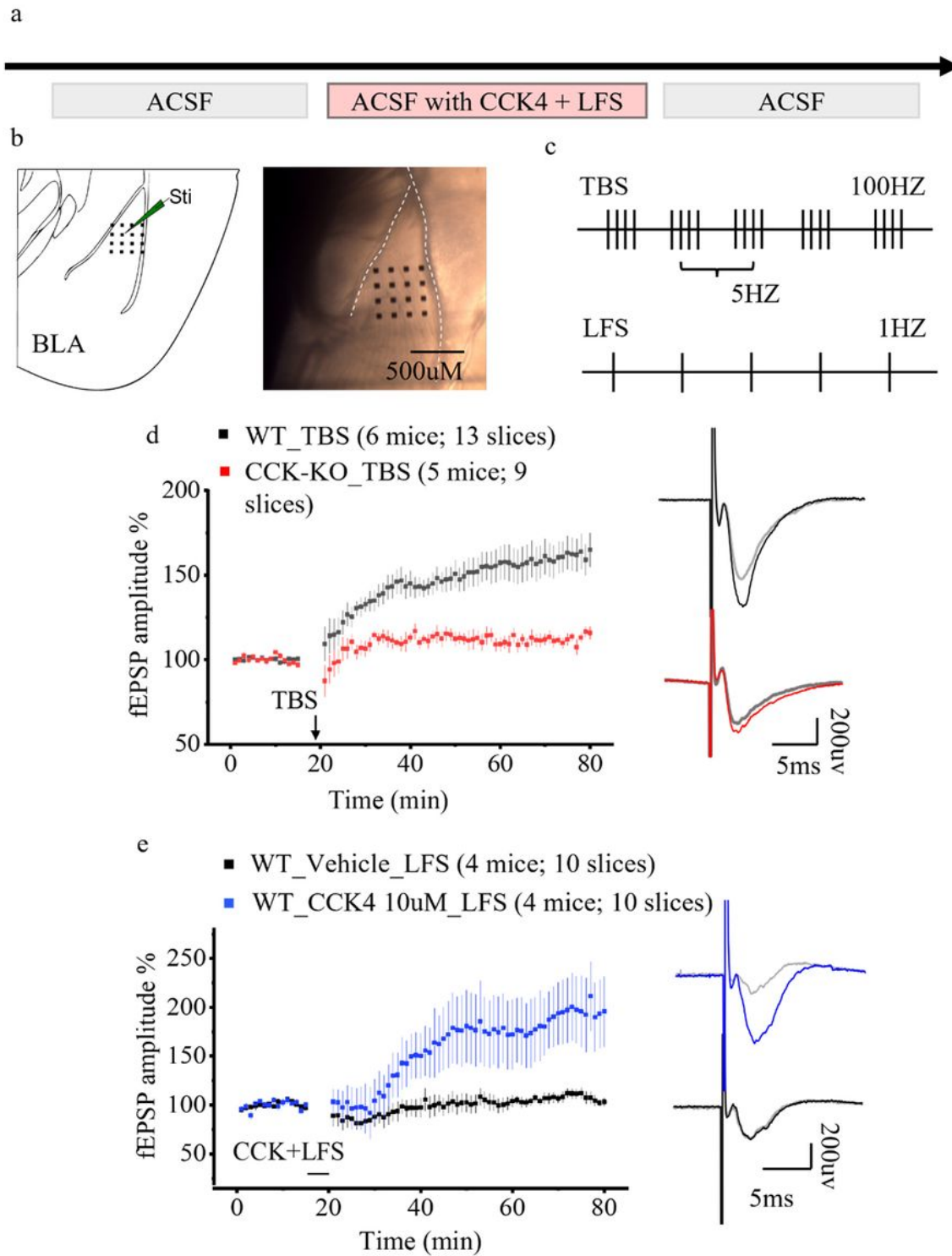
Figures

Figure 1

CCK signaling is critical in LTP induction in the BLA. a. Workflow of in-vitro recording and CCK4 administration, after 15min baseline recording, perfused artificial cerebrospinal fluid (ACSF) diluted with CCK4 for 5min with LFS, then fresh ACSF washed out CCK4 after. **b.** Light microscopy photograph showing the location of a 4*4 microelectrode array placed on the BLA region. **c.** Schematic diagram of TBS and LFS. **d.** Time courses of field excitatory postsynaptic potentials (fEPSPs) changes in response to TBS of wild-type mice (WT) and CCK-KO mice in the BLA (left). Representative fEPSPs traces before (gray) and after LTP induction (right). **e.** Time courses of fEPSPs changes in response to CCK4/vehicle with LFS in the BLA of WT mice (left). Representative fEPSPs traces before (gray) and after LTP induction (right). All data are the mean ± SEM.
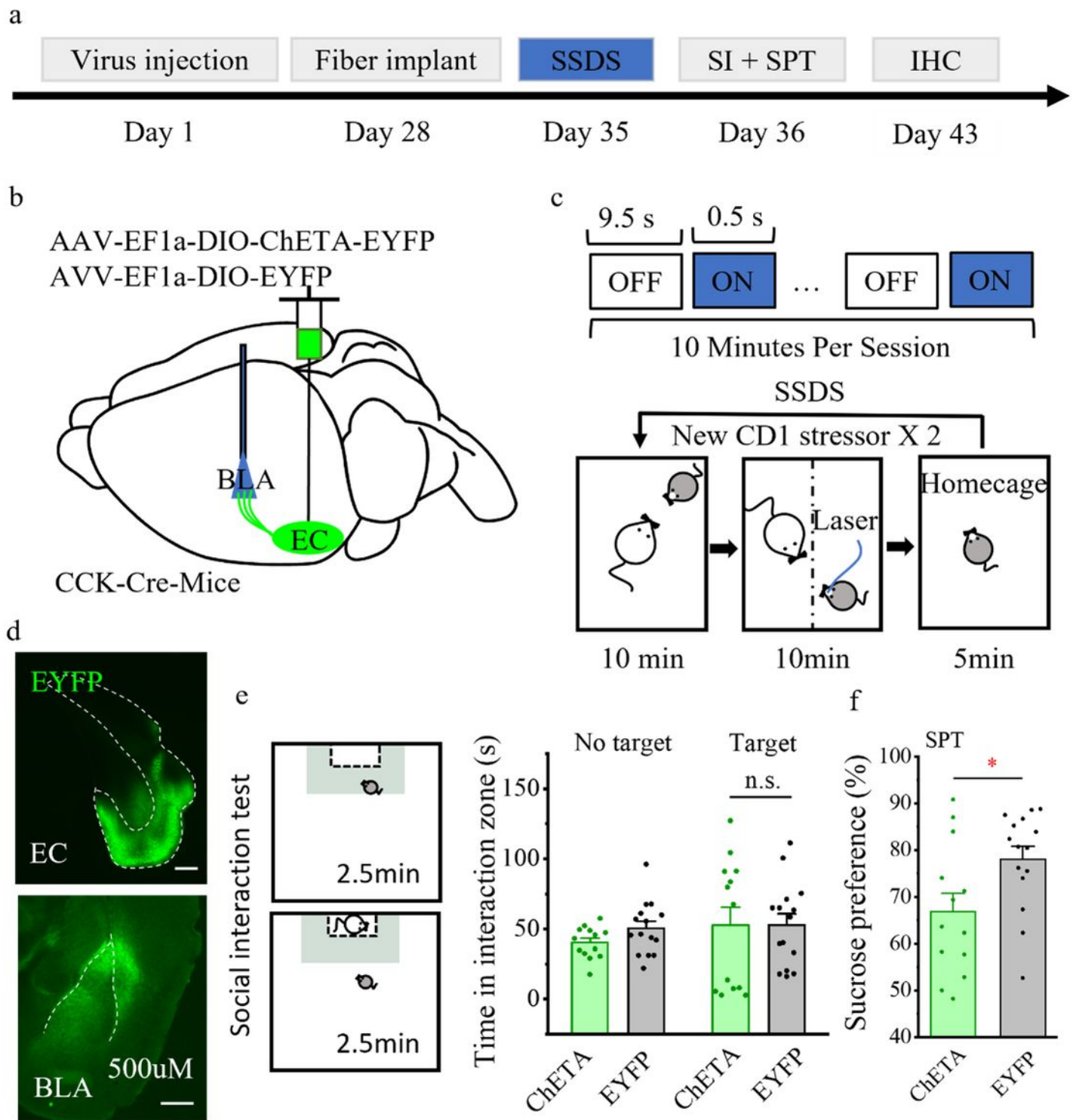
Figure 2

Optogenetic activation of the ECcck−BLA in SSDS induced depressive behaviors. a. The workflow of the SSDS model with optogenetic manipulation. Day 1, virus injection into the bilateral EC of CCK-Cre mice. Day 28, fibers implantation to the bilateral BLA. Day 35, SSDS paradigm with optogenetic activations. Day 36, SI, SPT. Day 43, BLA tissue collection for the immunohistochemistry (IHC) test. **b.** Schematic diagram of virus injection of EC and optical fiber implantation of BLA. **c.** Paradigms of 20 Hz optogenetic

activation of CCK fibers in the EC-BLA circuit during two sensory phases of SSDS. **d.** CHETA-EYFP or EYFP was specifically expressed in CCK neurons at EC (up) and projections to BLA (bottom), scale bar, 500 μm. **e.** Schematic diagram of SI (left). Time that mice spent in social interaction zone, two-way RM ANOVA, pairwise comparison, post hoc Bonferroni test (right). **f.** Sucrose preference percentage in the SPT, two-sample t-test. * P < 0.05, **P < 0.01, ***P < 0.001, n.s., not significant. All data are the mean ± SEM.
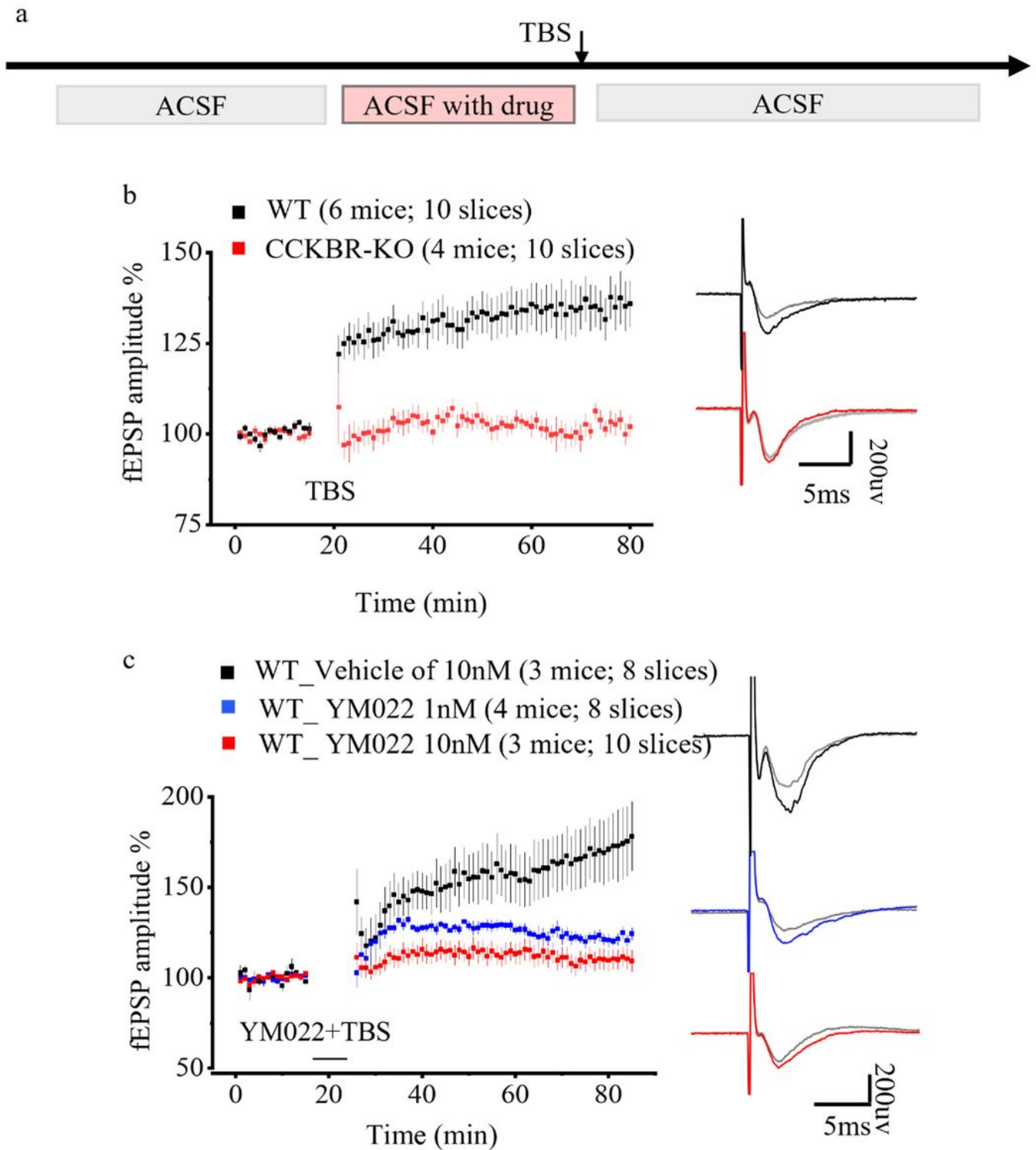
Figure 3

LTP deficit in CCKBR-KO mice and YM022 blocked LTP in the BLA. a. Workflow of in-vitro recording and drug administration, after 15min baseline recording, perfused ACSF diluted with drug for 10min, then fresh ACSF washed out drug after TBS. **b.** Time courses of fEPSPs changes in response to TBS of wild-type mice (WT) and CCKBR-KO mice in the BLA (left). Representative fEPSPs traces before (gray) and after LTP induction (right). **c.** Time courses of fEPSPs changes of C57 wild-type mice (WT) in response to

YM022/vehicle with TBS in the BLA (left). Representative fEPSPs traces before (gray) and after LTP induction (right). All data are the mean ± SEM.
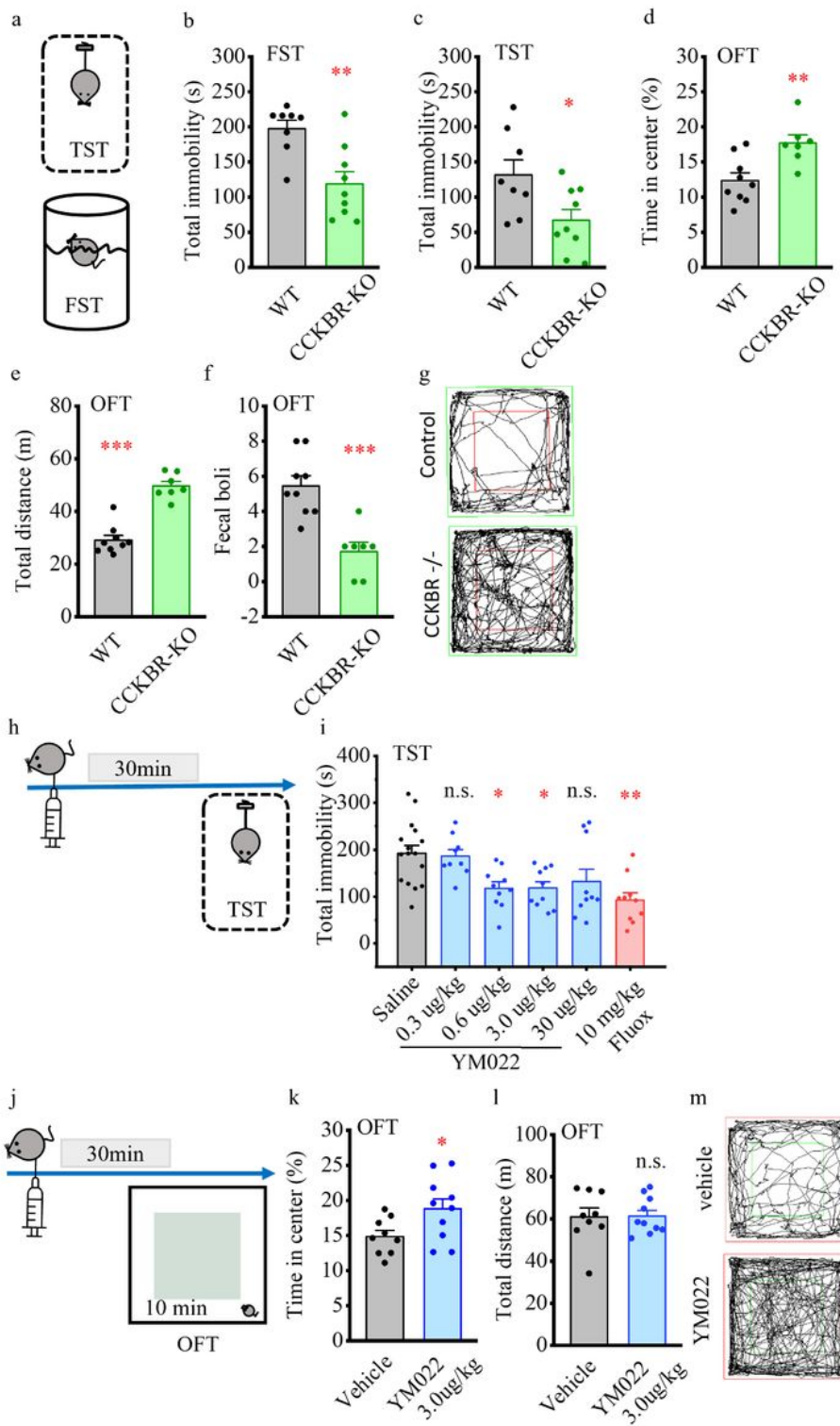

Figure 4

Antidepressant-related behavioral responses of CCKBR-KO mice and antidepressant effect of YM022 in acute stress model. a. Schematic of the TST and FST. **b.** Total immobility time in the last 4 min of the FST. wild-type mice (WT, N= 8) vs. CCKBR-KO mice (N=9), two-sample t-test. **c.** Total immobility time in 6 min of the TST, WT(N= 8) vs. CCKBR-KO (N=9), two-sample t-test. **d-g.** The anxiolytic behavior of CCKBR-KO mice (N=7) in the OFT, WT group (N=9). **d.** Time percentage spent in the center percentage, two-sample t-test. **e.** Total distance traveled, two-sample t-test. **f.** Fecal deposits, two-sample t-test. **g.** Representative traces in OFT (5min). **h.** YM022 administration 30 min before TST test by IP injection. **i.** Total immobility time in 6 min of the TST, saline group (N=16); YM022 groups, 0.3 μg/kg (N= 9), 0.6 μg/kg (N= 10), 3.0 μg/kg (N= 10), 30 μg/kg (N= 10), fluoxetine 10mg.kg (N= 10), one-way ANOVA, pairwise comparison, post hoc Bonferroni test. **j.** YM022 administration 30 min before the OFT test by IP injection. **k-m.** The anxiolytic effect of YM022 (3.0ug/kg, N=10) in the OFT, vehicle group (N=9). **k.** Time percentage spent in the center, two-sample t-test. **l.** Total distance traveled in the OFT, two-sample t-test. **m.** Representative traces in OFT (10min test time). * P < 0.05, **P < 0.01, ***P < 0.001, n.s., not significant. All data are the mean ± SEM.
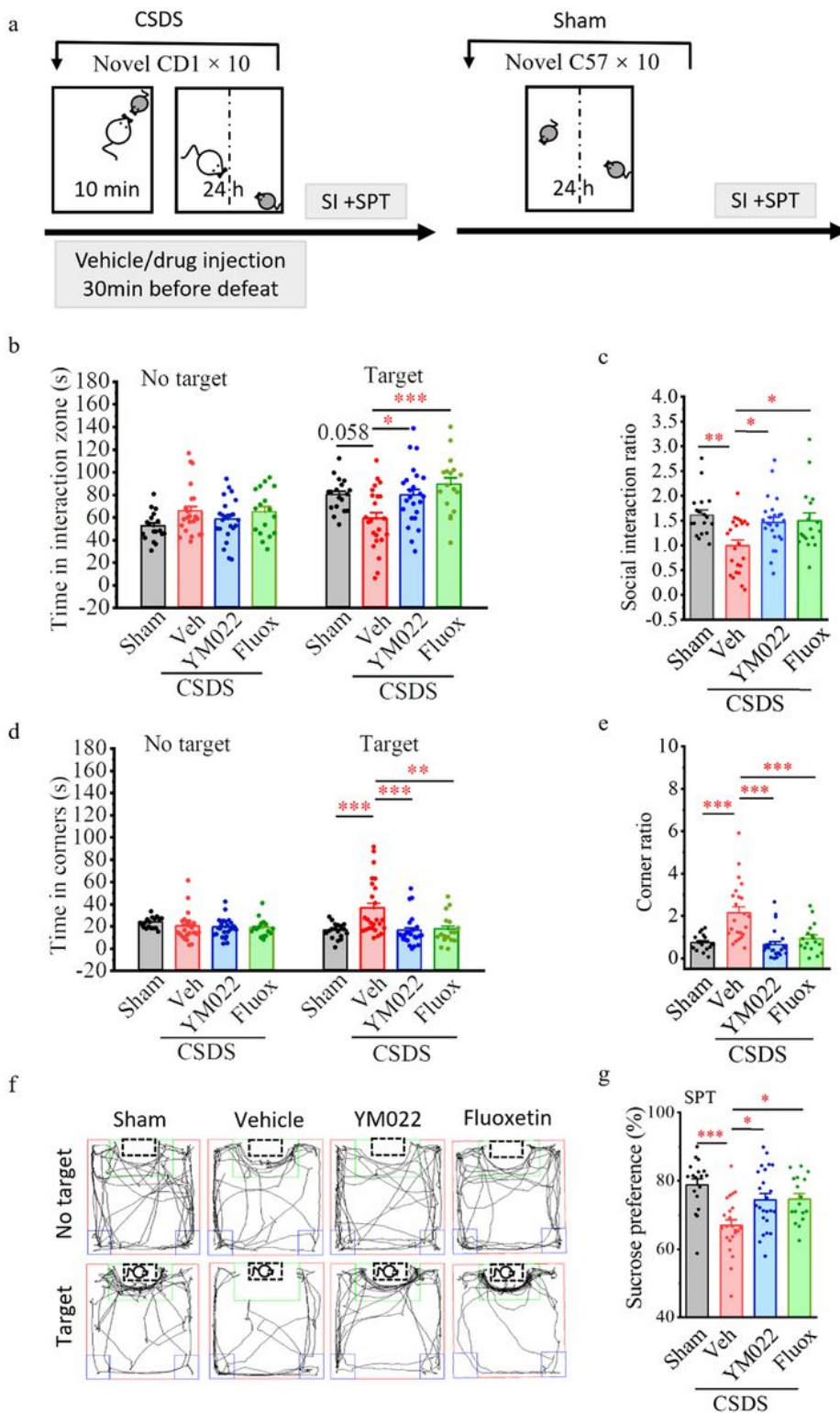
Figure 5

Antidepressant effects of YM022 in CSDS model. a. The workflow of CSDS with vehicle/YM022(3ug/kg)/fluoxetine(10mg/kg) injection 30min before every social defeat (left) and sham group(right). **b.** Time spent in social interaction zone in the absence and presence of a social target. Two-way RM ANOVA, pairwise comparison, post hoc Bonferroni test. **c.** Social interaction ratio = time spent in the social interaction zone with target/time spent in the social interaction zone without a target. One-way

ANOVA, pairwise comparison, post hoc Bonferroni test. **d.** The time that mice spent in corners in the absence and presence of a social target. Two-way RM ANOVA, pairwise comparison, post hoc Bonferroni test. **e.** Corner ratio = time spent in the corner with target/time spent in the corner without a target, One-way ANOVA, pairwise comparison, post hoc Bonferroni test. **f.** Representative sample track traces of social interaction test no-target phase (top), and the target phase (bottom). **g.** Sucrose preference percentage in SPT. One-way ANOVA, pairwise comparison, post hoc Bonferroni test. *P < 0.05, **P < 0.01, ***P < 0.001, n.s., not significant. All data are the mean ± SEM.

Supplementary Files

This is a list of supplementary files associated with this preprint. Click to download.

- Supplementaryfigure1.tif
- Supplementaryfigure2.tif
- Supplementaryfigure3.tif
- Supplementaryfigure4.tif
- Supplementaryfigure5.tif